

Nondestructive Quantification of Single-cell Nuclear and Cytoplasmic Mechanical Properties Based on Large Whole-Cell Deformation

Jifeng Ren^{a†}, Yongshu Li^{b†}, Shuhuan Hu^{acd}, Yi Liu^a, Sai Wah Tsao^e, Denvi Lau^f, Guannan Luo^g,
Chi Man Tsang^{b*}, and Raymond H. W. Lam^{ahi*}

^a Department of Biomedical Engineering, City University of Hong Kong, Hong Kong, China

^b Department of Anatomical and Cellular Pathology, Chinese University of Hong Kong, Hong
Kong, China

^c BGI-Shenzhen, Shenzhen 518083, Guangdong, China

^d Guangdong High-Throughput Sequencing Research Center, Shenzhen, Guangdong, China

^e School of Biomedical Sciences, The University of Hong Kong, Hong Kong, China

^f Department of Architecture and Civil Engineering, City University of Hong Kong, Hong Kong,
China

^g Department of Economics and Finance, City University of Hong Kong, China

^h City University of Hong Kong Shenzhen Research Institute, Shenzhen, China

ⁱ Centre for Biosystems, Neuroscience, and Nanotechnology, City University of Hong Kong,
Hong Kong, China

* Correspondence should be addressed to RHW Lam (email: rhwlam@cityu.edu.hk; Tel: +852-3442-8577; Fax: +852-3442-0172) and CM Tsang (email: annatsang@cuhk.edu.hk).

† These authors contributed equally to this work.

Electronic Supplementary Information (ESI)

3D nuclear shapes of NP460 and NPC43 cells

To further verify whether nuclei of NP460 and NPC43 cells are substantially spherical shapes, we applied laser confocal microscopy to obtain 3D images of Hoechst 33342 stained nuclei. Briefly, we utilized scanning process on a fluorescent nucleus from the top to bottom with many planes (typically ~100 planes scanned) on a laser confocal microscope and then 3D view of stained nucleus can be generated. As shown in **Fig. S1a** and **Fig. S1b**, nuclei of both NPC43 and NP460 present roughly spherical shapes. Therefore, considering nuclei of NPC43 and NP460 as soft spheres can obtain measuring results with less errors.

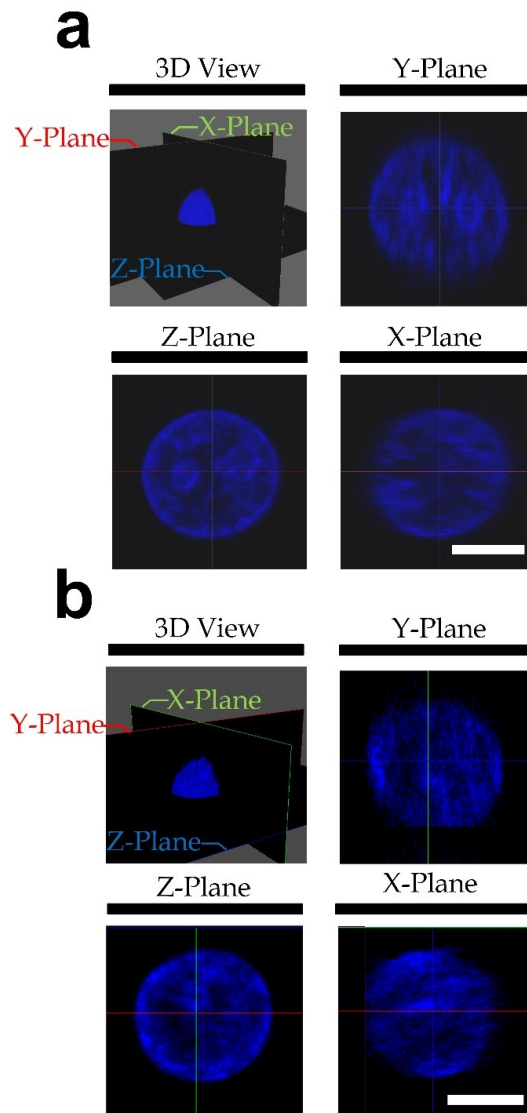


Figure S1. 3D view and nuclear shapes on different cross-sections of Hoechst 33342 stained (a) NPC43 and (b) NP460 cells. Scale bar: 10 μm .

Effective pressure difference on single confining microchannels

To study the effective pressure difference driven on a single confining microchannel, we divided the total microfluidic device into several flow sections. As illustrated in **Fig. S2a**, the whole device can be considered as consisting of a main flow section (R_m), four bypass channels (R_1, R_2, R_3, R_4), and a downstream outflow channel (R_{out}). Therefore, we can calculate effective pressure differences on each flow section by considering circuit model of flow resistances.¹ The whole microfluidic device flow resistance can be considered as main flow section paralleled connected with four bypass channels and then together series connected with an outflow channel as shown in **Fig. S2b**. The flow resistances can be calculated by:

$$R = \frac{\bar{p}}{S} \quad (\text{S1})$$

where R is the flow resistance of flow section, \bar{p} is the average pressure in flow section, and S is integrated flow rate in flow section.

After implementing COMSOL Multiphysics 5.2a (Burlington, MA) to calculate average pressures and flow rates for all flow sections, we can obtain flow resistances of flow sections by using **Eqn. S1** as shown in the table below:

Table S1. Calculated flow resistances of every flow section in the microfluidic device.

	R_m	R_1	R_2	R_3	R_4	R_{out}
Flow Resistance (Pa·s/m ³)	5.57×10^9	6.89×10^{10}	6.87×10^{10}	6.09×10^{10}	6.11×10^{10}	1.29×10^7

The total flow resistance of the paralleled connected group R^* can be calculated by:

$$\frac{1}{R^*} = \frac{1}{R_m} + \frac{1}{R_1} + \frac{1}{R_2} + \frac{1}{R_3} + \frac{1}{R_4} \quad (\text{S2})$$

By substituting values of **Table S1** in **Eqn. S2**, we can obtain $R^* = 4.14 \times 10^9$ Pa·s/m³. After considering the pressure distributions according to the flow resistances, the effective pressure difference of the main flow section is

$$P_{eff} = P_{drive} \cdot \frac{R^*}{R^* + R_{out}} = 99.69\% \cdot P_{drive} \quad (\text{S3})$$

where P_{eff} is the effective pressure difference of the main flow section, P_{drive} is the driving pressure applied on the whole microfluidic device. Because every confining microchannels are parallel connected in main flow section, their pressure differences between inlets and outlets should be much similar as the flow section pressure. Therefore, we can approximately consider the pressure values of on the pressure reducing regulator as the pressure differences between each confining microchannels.

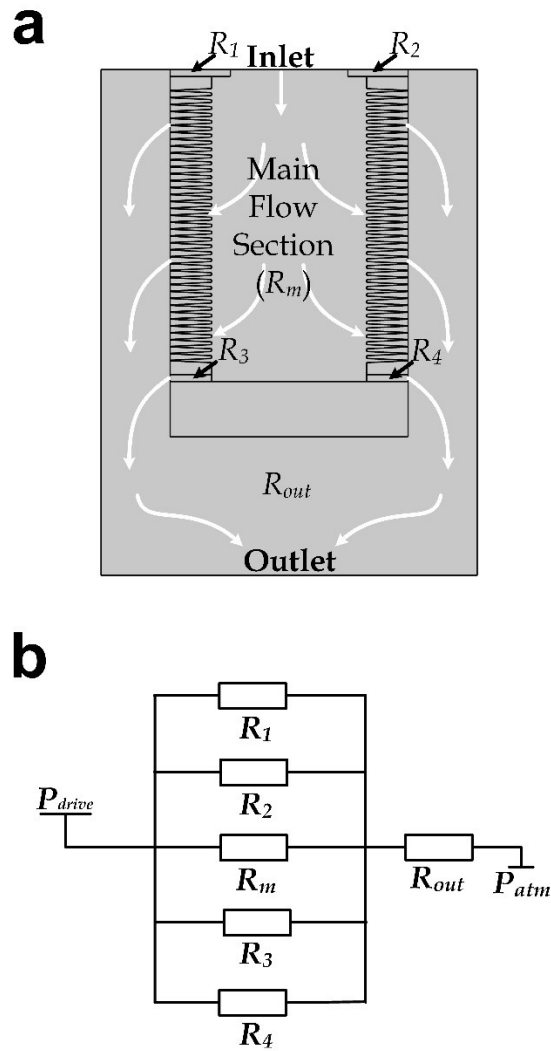


Figure S2. (a) Diagram of the flow sections in whole microfluidic device. (b) Circuit model of flow resistances distributions for flow sections (P_{atm} is the atmospheric pressure).

Nuclear size and elasticity distributions of measured NP460 and NPC43 cells

To discover the feasibility of classifying NPC43 cells from NP460 cells using their nuclear diameters and elasticities, we firstly counted their nuclear diameter distributions and nuclear elastic moduli distributions separately. As shown in **Fig. S3**, it is obvious that significant distribution difference can be found between two cell lines in both nuclear diameter and nuclear elasticity. For nuclear diameter distributions, NP460 cells centralize in the group ranging from 8 μm to 12 μm while NPC43 cells tend to distribute in group ranging from 12 μm to 14 μm . If we take nuclear diameter value of 12 μm as the nuclear size separating boundary, there will be 64.6 % NPC43 cells in the ‘larger’ domain and 87.2 % NP460 cells in ‘smaller’ domain. And when considering the nuclear elasticity, majority of measured NPC43 cells own nuclear elasticities

ranging from 2 kPa to 4 kPa while a large number of measured NP460 have nuclear elasticity ranging from 4 kPa to 6 kPa. If we take nuclear elastic modulus value of 4 kPa as the nuclear stiffness separating boundary, there will be 62.5 % NPC43 cells in ‘softer’ domain and 78.7 % NP460 cells in ‘stiffer’ domain.

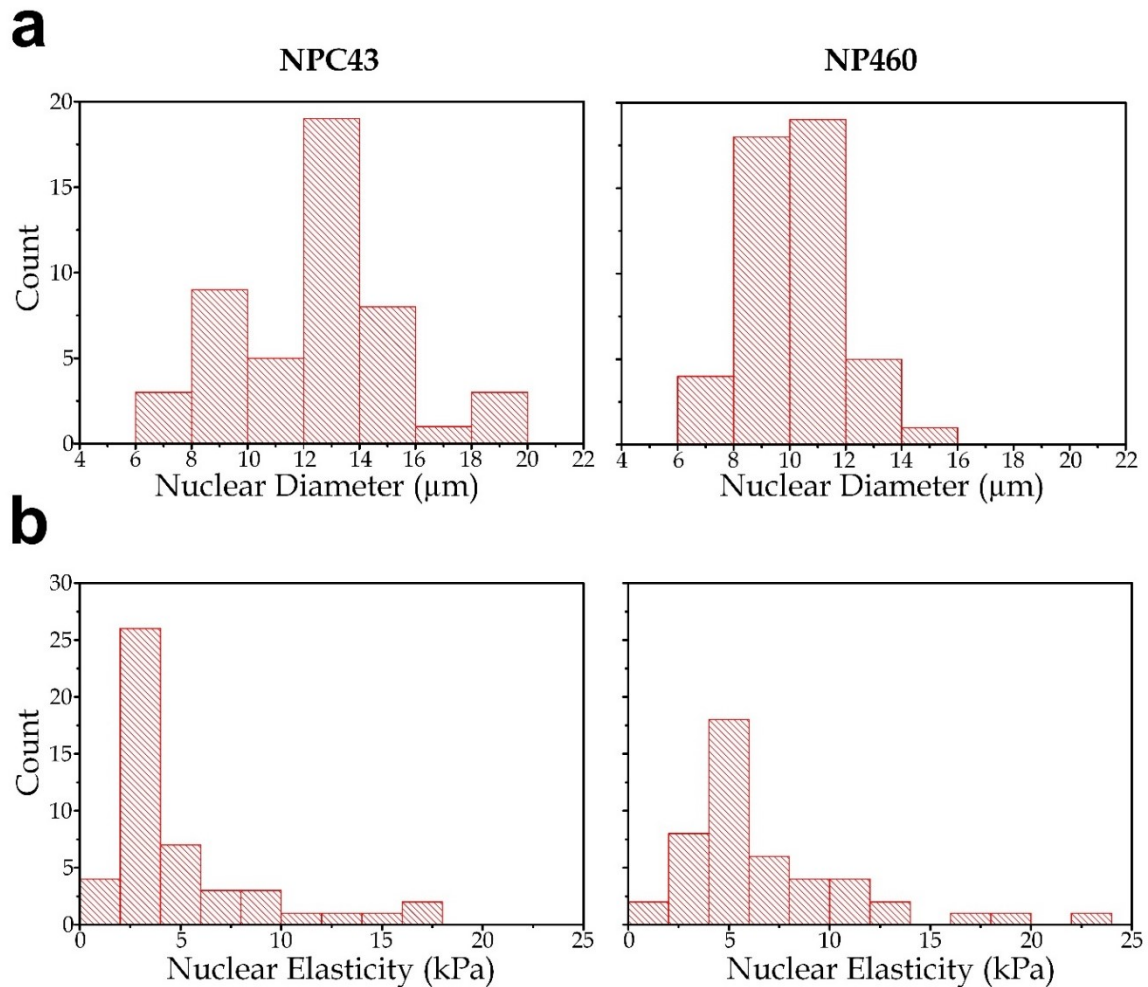


Figure S3. (a) Nuclear diameter distributions of measured NP460 and NPC43 cells. **(b)** Nuclear elasticity distributions of measured NP460 and NPC43 cells.

Reference

1. S. Hu, and Raymond HW Lam, *Microfluidics and Nanofluidics*, 2017, **21**, 68.